

Research Article

Challenges in Circumferential Entry Blades for Structural Integrity of Closing Blade in Steam Turbines

A S Suresh Babu^{†*}, Jeevan Gowda G[‡] and M V Reddy[†]

[†]Mechanical Engineering Department, VTU, Ghousia Engineering college Ramanagara India

[‡]Mechanical Engineering Department, Kshipra Simulations Pvt Ltd, Nagarabhavi Bangalore India

[†]Mechanical Engineering Department, VTU, BIT Bangalore India

Received 14 April 2018, Accepted 15 June 2018, Available online 22 June 2018, Vol.8, No.3 (May/June 2018)

Abstract

The bladed disc of an LP last stage rotor assembly in a steam turbine often employs circumferential entry blades. The closing blade is fastened with the aid of a pin type locking mechanism, which locks the closing blade onto the disc. Radial entry blade root design demands for a groove in the disc through which blades are inserted and guided to their respective final positions which alters the stiffness in the disc. Closing blade is the most highly stressed weak link zone in the circumferential entry rotor disc achieving mechanical integrity for in-service condition is a challenge. Location of pin and its insertion is the key to achieve the desired in-service life with good material model. The present research work focus on emphasis of pin positioning to lock the T-root blade at operating range. Various material model configurations and pin positions are considered in both blade and disc to improve the reliability in design. Customized methodology is developed to address the elasto-plastic kinematic hardening in pin, disc and blade groove during in-service life. Finite element approach along with classical design equations followed by API 616 standards is employed to achieve the mechanical integrity in bladed disc assembly.

Keywords: LP stage rotor, steam turbine, centrifugal load, locking pin, closing blade, over speed.

Introduction

Blade failure can be seen in steam turbines often due to the increase in mass flow rate of steam at LP stage, rotor over speeding and manufacturing uncertainties. Such failures result in economic penalties to the affected utilities like blades, disc, nozzle, casing and so on (Poursaeidi and Mohammadi *et al*, 2008). Circumferential entry type rotor discs are preferable when compared to axial entry bladed discs, as they are designed to withstand high centrifugal forces without the risk of all blades leaving the rotor. This is because in axial entry blades, each blade needs a locking mechanism to hold the blade from moving radially whereas in circumferential entry blades, only closing blade is the weak link in the rotor. Therefore, if closing blade is designed for its robustness, the need of locking mechanism for every blade is not necessary. Structural failures in circumferential entry bladed rotors have been commonly seen to occur due to poor design considerations of the locking pin which holds the final closing blade along with the other adjacent blades together. Inconsistency and errors in manufacturing/assembly also lead to the rotor having significantly lower safety margins. Since, steam

turbines have a wide range of applications in industrial power generation, their efficient operating conditions for an extensive period of time is crucial.

The other problems that encountered in closing blade is eccentricity of hole and pin, fretting, fatigue, vibration, low flow rate. Eccentricity is a condition of loading in which the point of action of load is not on the neutral axis of hole/pin. Whenever there is eccentric loading there starts the effect of combined direct and bending stresses.

Fretting refers to wear and sometimes corrosion damage at the asperities of contact surfaces. This damage is induced under load and in the presence of repeated relative surface motion, as induced for example by vibration. Fretting decreases fatigue strength of materials operating under cycling loading (Sharma and Joshi *et al*, 2001). This can result in fretting fatigue, whereby fatigue cracks can initiate in the fretting zone. Afterwards, the crack propagates into the material. Experimental work is carried at material testing lab to correlate the FE results for double shear component for benchmarking.

This paper deals with the positioning of locking pin and investigations of various uncertainties such as eccentricity of pin/hole, operating speeds and over speed margin of the rotor. High centrifugal forces are often a contributing factor to consequent failure of the

*Corresponding author's ORCID ID: 0000-0003-3881-9989
DOI: <https://doi.org/10.14741/ijcet/v.8.3.34>

locking pin. Various configurations for location of the pin is being established while portraying various contributing factors such as contact stresses (stress generated at areas where two or more bodies interact with each other) and bending stresses being generated in the rotor.

Locking Mechanism in Circumferential Entry Blade

The general appearance of a two-pin mounted closing blade is shown in figure 1. Here a closing blade having two locking pins is shown. However, this may not hold true for other cases since the number of pins depend on the centrifugal force of the blade at in-service condition, trying to shear the pin.

The T - root closing blade is plugged at the slot crated in the rotor for inserting and guiding the moving blades. Locking pins are inserted between the closing blade and adjacent moving blades.

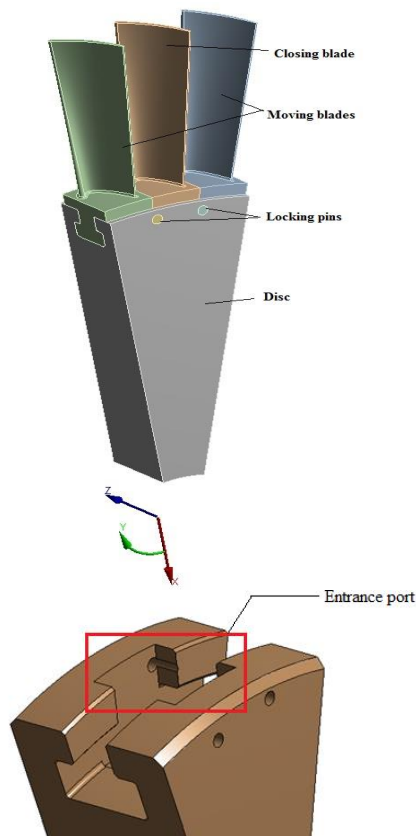


Figure 1: Closing blade and locking pin configuration

The assembly of closing blade and locking pin is as shown in figure 1. Closing blade is the final blade that is inserted onto the rotor. This blade carries a relatively higher mass than the adjacent blades, since material loss due to presence of holes on either sides of neck region in the closing blade will result in loss of stiffness and this loss needs to be compensated by increasing the mass of closing blade. The increase in mass will reduce radial growth of pin, which develops friction between blade tip and casing. This friction can be reduced by providing necessary coating to blade tip.

Contacts exist between the locking pins and closing blade. These contacts are treated as frictional contacts having coefficient of friction 0.2. There are contacts generated between the blade platforms of closing blade and adjacent blades. These contacts are also treated as frictional contacts with coefficient of friction being 0.2. The locking pins are inserted into the closing blade assembly and a fit is achieved between these bodies through shrink fit. The type of fit achieved between the closing blade and adjacent blades is through tolerance fit. Tolerance of ± 10 microns is provided on either sides of the closing blade platform (Jafarali, Krikunov *et al.* 2012). The stresses created by the steam pressure, centrifugal forces caused by the spinning of the bladed rotor, and the unavoidable vibration resulting in the blading make shot peening *et al* margin between failure and success to an impressive degree.

The other problems that encountered in closing blade is eccentricity of hole and pin, fretting, fatigue, vibration, low flow rate. Eccentricity is a condition of loading in which the point of action of load is not on the neutral axis of hole/pin (Banaszkiewicz *et al.*, 2014). The effect of eccentricity causes variation of parallelism in pin which leads to uneven loading on locking pins. The edge distance between rotor and locking is shown in figure 1. The decrease in edge distance will decrease the bearing area between pin and disc which intern increases bearing stress, contact stress at the disc pin interface.

Achieving mechanical integrity of locking blade assembly of design life is a challenge. The material used for blades and rotor is chromium steel (XCrmov55) (Rao, Peraiah *et al.*, 2009) which is extensively used in manufacture of steam turbine rotors as they are highly corrosion resistant and creep resistant. Similarly, material used for the locking pin is titanium alloy (Ti-6Al-4V) (Jaffee *et al.*, 1990) which has high strength, low weight ratio and corrosion resistance. The analysis is performed by allocating relevant material properties to components, also considering nonlinearities in geometry and material.

Friction Contact Modelling

The contacts generated in this assembly are all considered to be of frictional type. An isotropic friction model is used in this case which employs a single coefficient of friction μ_{iso} based on the assumption of uniform stick-slip behavior in all directions. From basic Coulomb friction model considered for FE analysis, two contact surfaces can carry shear stresses. When the equivalent shear stress is less than a limiting frictional stress τ_{lim} , there is no motion between the two contact surfaces. This phenomenon is known as sticking. Coulomb friction model is defined as: $\tau_{lim} = \mu P + b$

$$||\tau|| \leq \tau_{lim}$$

Where,

$$\tau_{lim} = \text{Limit frictional stress}$$

$$||\tau|| = \sqrt{\tau_1^2 + \tau_2^2} \text{ equivalent stress (for 3-D contact elements)}$$

μ = coefficient of friction for isotropic friction
 P = normal contact pressure
 b = contact cohesion

After the equivalent frictional stress has exceeded τ_{lim} , the contact and target surfaces will slide relative with each other. This phenomenon is known as sliding. Figure 2 represents the friction model with respect to sticking and sliding.

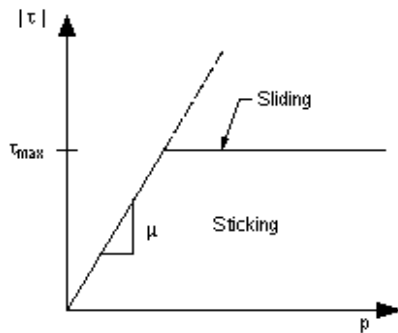


Figure 2: Friction model

The friction element geometry for the present is portrayed in figure 3 where R and S axis of the applicable co-ordinate system. Friction element is used to represent contact and sliding between two 3-D target surfaces and a deformable surface defined by eight nodes. is an 8-node element that is intended for general rigid-flexible and flexible-flexible contact analysis and is used to represent contact and sliding between 3-D surfaces. The element is applicable to 3-D structural and coupled field contact analyses. It can degenerate to a six node element depending on the shape of underlying solid elements. Frictionless behavior allows the bodies to slide relative to one another without any resistance. When friction is included, shear forces can develop between the two bodies. Frictional contact may be used with small-deflection or large deflection analyses.

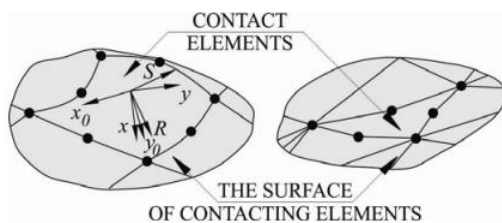


Figure 3: Contact Element

The contact element allows the use of both isotropic and orthotropic friction models. In this case an isotropic friction model was used with a variable coefficient ranging between 0.35 and 0.55 and a starting value of 0.45 that corresponds to the coupling materials determined experimentally.

For the finite element, the rate of frictional dissipation is evaluated using the frictional heating factor and is given by

$$q = FGTH\tau V \tag{1}$$

where: τ is the equivalent frictional stress,
 V - the sliding rate and
 FGTH - the fraction of frictional dissipated energy converted into heat (the default value of 1 was used for this parameter).

The amount of frictional dissipation on contact and target surfaces is given by

$$q_c = FwFftv \tag{2}$$

$$q_T = (1 - Fw)Fftv \tag{3}$$

where: q_c - The amount of frictional dissipation on the contact side,
 q_T - The amount of frictional dissipation on the target side and
 FWGT is a weighted distribution factor (the default value of 0.5 is used for this parameter).

The relationships presented previously are valid only for the sliding mode of friction and a coefficient of friction greater than zero.

Load Considerations in Circumferential Entry Rotor Blade

The complete circumferential entry rotor disc and its components are subjected to high rotational velocities, which is a body force. The rotational velocity has an impact on other loading conditions, as bending loads and shear loads are imparted on the locking pins and the closing blade. Shear loads are also prominent along the length of the pins and across the cross section of the pins. However, possibilities of all manufactural uncertainties like parallelism of locking pin, contact uncertainties like sticking, sliding, partial contact across the length of locking pin. Whenever there is eccentric loading there starts the effect of combined direct and bending stresses. The effect of these loads on the closing blade and locking pin are therefore investigated through Nonlinear kinematic finite element simulation and customized methodology for theoretical calculations for all design purpose. The design rule margins are necessary for uncertainties present in material, manufacturing, assembly and on site operating conditions.

- Yield strength at room temperature = 585 MPa
- Yield strength at operating temperature (500) = 575 MPa
- Factor of safety at operating speed = 1.68
- Factor of safety at over speed = 1.15 (Tulsidas, Shantharaja et al, 2012)
- Allowable stress at operating speed:

$$\sigma_{allowable} = \frac{\sigma_{minimum}}{overspeed^2 * FOS}$$

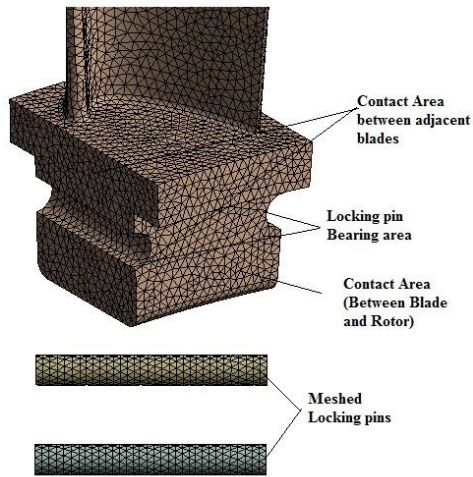


Figure 4: Contact regions in the closing blade

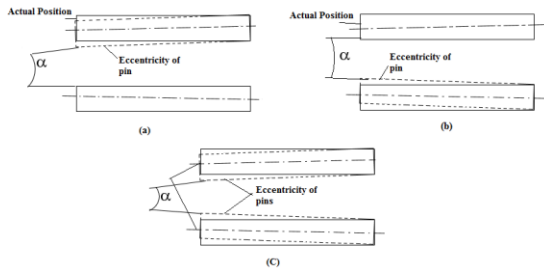


Figure 5: Eccentricity of locking pin

The interactions between blade platforms, the locking pin and closing blade area of contact, the blades and rotor sliding region are existing under service condition. These junctions of contact, as shown in figure 4 (bodies not to scale) are considered as sensitive contact regions which are subjected to frictional resistance during operation of the turbine. Hence contacts have to be suitably provided with appropriate friction models defined at each location for simulation purposes by updating stiffness for each and every iteration.

The angle α as shown in figure 5 symbolizes the eccentricity of locking pin. The angle α should be equal to zero, hence the load acting on the pin will distribute among locking pins. The eccentricity of pin occurs during assembly due to manufacturing error or variation in tolerances provided resulting in discounting of in-service life.

Objectives and Scope of Work

The main objective of this work is to develop a simulation model of the closing blade and locking pin assembly and conduct sensitivity checks for the bladed disc integrity. Locking pins help in locking the closing blade which is the final blade being inserted into the rotor.

Being a crucial part in the locking system for the blades, its failure can prove disastrous. The pin is subjected to lateral bending as it holds the closing blade which is subjected to centrifugal loading due to which it tends to displace in the radial direction. If the bending stresses generated tend to be high, yielding of the pin is inevitable.

Although two locking pins are employed for the locking mechanism in the assembly, it may sometimes not be enough to withstand high and uncertain over speeds.

A comprehensive presentation of all possible design modifications is established through sensitivity analysis blending the classical approach with simulation engineering to arrive at best possible solution replicating the physical conditions. Computed engineering analysis could be the best possibility for arriving better clarity at design feasibility during in service conditions.

Numerical Investigation and Simulation Methodology

Structural analysis is conducted for the closing blade assembly for different loading conditions, the geometric variable being the locking pin position. Analysis is also carried out for two different configurations for emplacement of locking pins along the radial direction.

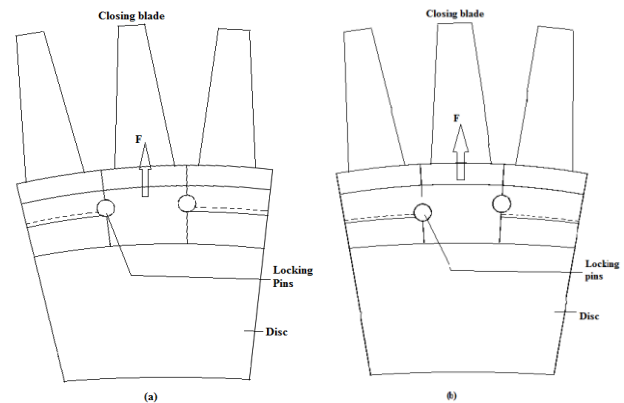
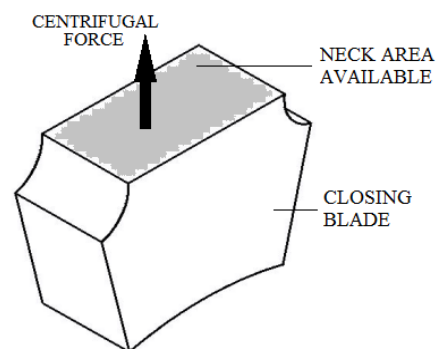


Figure 6: Locking pin arrangement (a) Configuration 1 (b) Configuration 2



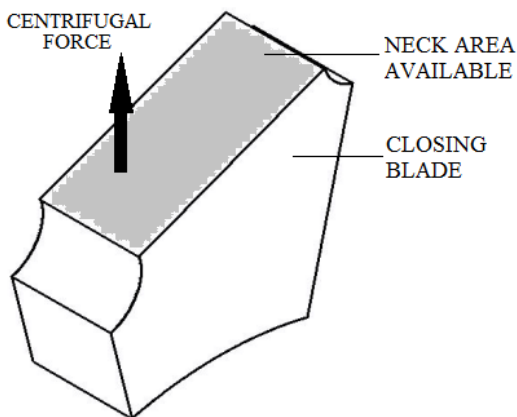


Figure 7: Cross sectional area across reference curve in closing blade (a) Configuration 1 (b) Configuration 2

In configuration 1 as shown in figure 6a centers of both pin 1 and pin 2 lie on the same reference curve. For this type of configuration, there is a decrease in neck area of the blade (as shown in figure 7a). However, in configuration 2, pin 1 and pin 2 are placed in a criss-cross fashion on two different reference curves as depicted in figure 6b. In this configuration the neck area of the blade available is comparatively higher by 11% that of configuration 1 (as shown in figure 7b). The availability of adequate neck area is emphasized as drastic reduction in neck area will result in failure of the closing blade due to increase in section stress (Average stress at the cross sectional area of a body) at that region.

Classical approach for sizing of locking pin:

$$\text{Yield Stress, } \sigma_y = Fc/A \text{ N/mm}^2$$

Where, σ_y = Yield strength of titanium alloy = 880 MPa

$$\text{Centrifugal force, } Fc = m\omega^2r$$

Where, m = mass of closing blade = 0.53559 Kg

$$\omega = \frac{2\pi N}{60} \text{ rad/sec}$$

r = centre of gravity = 0.419 m

Cross sectional area of locking pin, A = 4A (because, shear of locking pin occurs at 4 regions)

Therefore, diameter of pin = d = 8mm.

Two pins of diameters 8 mm are taken for simulation for which both of them are analyzed for strength and stresses separately. The neck region of closing blade is a highly stressed as centrifugal loads tend to act directly. Since, the integrity of the locking pins is vital, section stresses at critical locations needs to be below the allowable design stress. Else, failures due to excessive bending and fatigue are inevitable. The results obtained from this simulation are shown in figure 8.

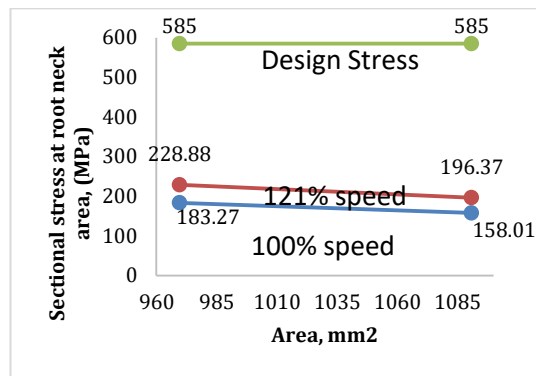


Figure 8: Gross Yielding stress at blade root neck

It is observed, that section stress at the blade root neck region of configuration 1 is 183.27 MPa whereas for configuration 2 section stress is 158.01 MPa. This result portrays that as the pin diameter increases, the bearing area on the closing blade decreases due to which there is a dip in stress levels (as area tends to increase, the stress correspondingly decrease). Similarly, in case of over speed (121% speed) the gross yielding stress at the blade root neck region of configuration 1 is 228.88 MPa whereas for configuration 2 section stress is 196.37 MPa.

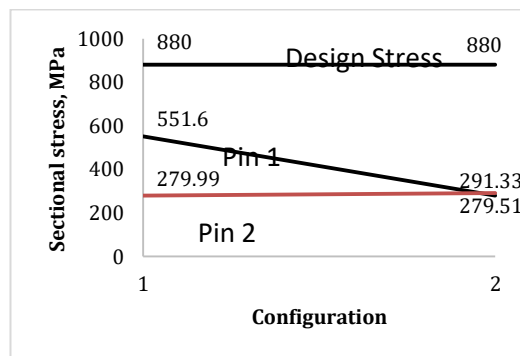


Figure 9: Gross Yielding stress of locking pin

In figure 9, the gross yielding stress in locking pin 1 of configuration 1 is 551.6 MPa and 279.51 MPa for configuration 2. Similarly, the section stress in locking pin 2 of configuration 1 is 279.99 MPa and 291.33 MPa for configuration 2. This dip in average section stress is due to the increase of neck cross sectional area. Therefore, it is evident that the locking pin of configuration 2 is more structurally prominent when compared to a locking pin of configuration 1.

Analytical Verification

Shear stress is the most common failure method for locking pins as they act as a weak link in the closing blade structure. However, there have been cases of pins failing despite being adequately sized for shear. This may be due to negligence of taking into account pin bending as a legitimate failure mode. Based on simple shear stress equations, the locking pin and

closing blade are investigated and validated through finite element analysis.

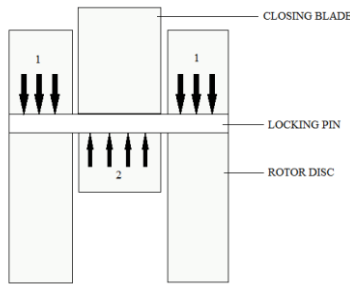


Figure 10: Load distribution across the locking pin

For a closing blade due to its weak link analogy, load distribution across the locking pin is as shown in figure 10 where:

Load 1 shows variable reactive loads due to the resistance offered by rotor disc.

Load 2 shows variable load distribution across center of the locking pin due to centrifugal force exerted on the closing blade.

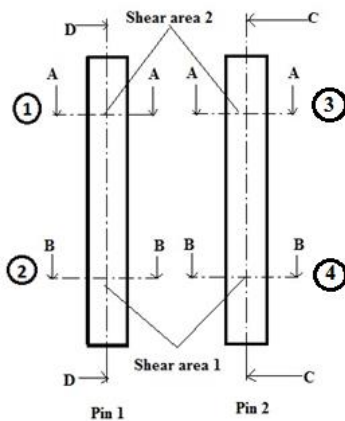


Figure 11: Gross yielding stress at cross sectional area of the locking pin

$$\text{Stress, } \sigma_y = \frac{F_C}{A} \text{ N/mm}^2$$

$$\text{Centrifugal force, } F_c = m\omega^2 r$$

Where, m = mass of closing blade = 0.53559 Kg

$$\omega = \frac{2\pi N}{60} \text{ rad/sec} = \frac{2 * \pi * 8650}{60} = 905.82 \text{ rad/sec}$$

r = centre of gravity = 0.419 m

Gross yielding stress in cross section of pin:

$$F_c = m\omega^2 r = 0.53559 \times 905.822 \times 0.419 = 184134.82 \text{ N}$$

$$A = \frac{\pi d^2}{4}$$

FOS, Factor of safety = 1.68

$$\text{Stress, } \sigma_y = \frac{F_C}{4A} = \frac{184134.82}{201.06} = 915.81 \text{ N/mm}^2$$

Longitudinal shear of pin at cross section D-D and C-C:

$$\text{Longitudinal shear } \tau_{pin} = \frac{F_C}{2A} = \frac{184134.82}{960} = 191.81 \text{ N/mm}^2$$

Shear stress of pin between A-A and B-B:

$$\text{Shear stress } \tau_{pin} = \frac{F_C}{2A} = \frac{184134.82}{2 * 271.39} = 339.24 \text{ N/mm}^2$$

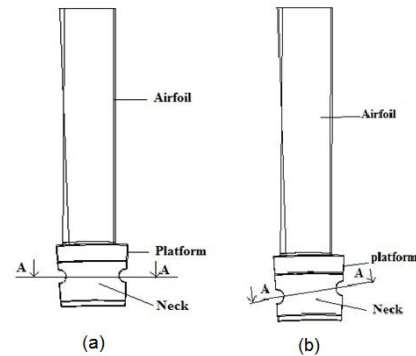


Figure 12: Gross yielding stress at cross sectional area of neck area

Gross yielding stress at cross sectional area of neck region:

$$\text{Stress, } \sigma_y = \frac{F_C}{A} = \frac{184134.82}{969.53} = 189.92 \text{ N/mm}^2 \text{ (Cross sectional area at A-A in figure 14a)}$$

$$\text{Stress, } \sigma_y = \frac{F_C}{A} = \frac{184134.82}{1090.81} = 168.80 \text{ N/mm}^2 \text{ (Cross sectional area at A-A in figure 14b)}$$

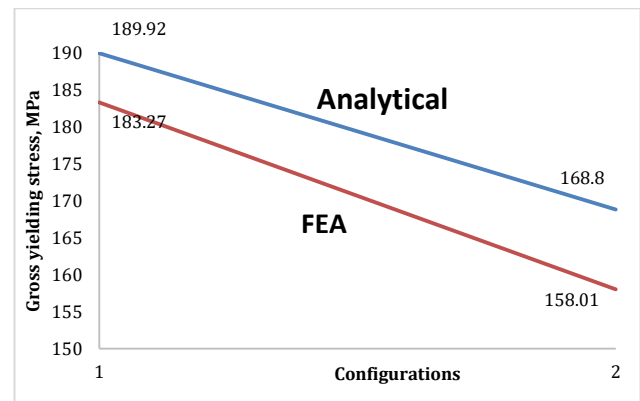


Figure 13: Gross yielding stress at cross sectional area of neck region

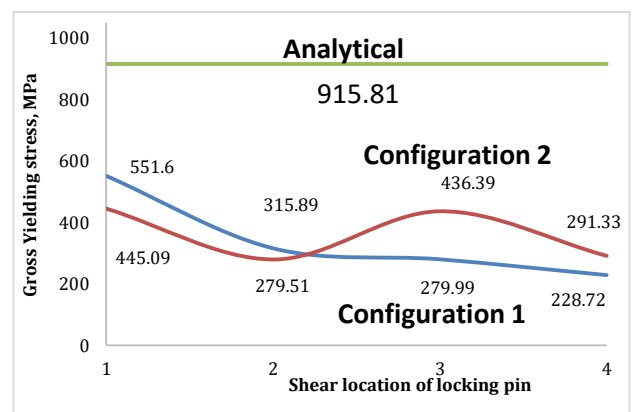


Figure 14: Gross yielding stress at shear area of Locking pins

Figure 14 shows the graphical representation of Gross yielding stress at different cross sectional area of the locking pins as shown in figure 11. The peak stress in locking pin is 551.6 MPa. however, the structural integrity of locking pin is achieved with the FOS of 1.6. The variation of gross yielding stress of classical approach from FEA is due to material non linearity, bilinear kinematic hardening, manufacturing uncertainties which are not considered in classical approach.

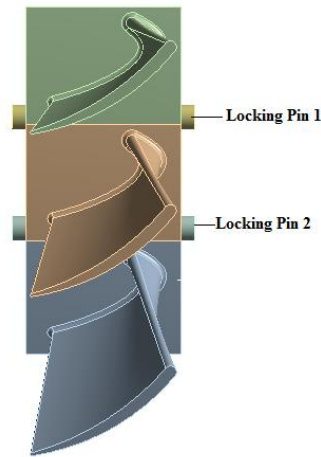


Figure 15: Top view of locking pins and closing blade

To make the analysis more viable for durability estimation, the locking pins of two different configurations are considered and section stress along the length of the pins is compared. Let us consider two pins, pin 1 and pin 2 as shown in figure 15.

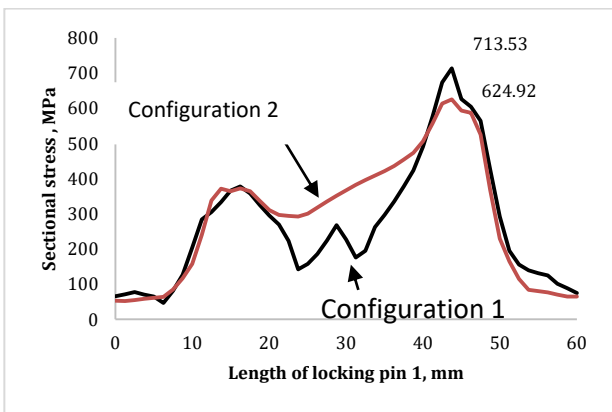


Figure 16: Section stress along the length of locking pin 1

Figure 16 portrays the variation of section stress taken along the length of the locking pin 1 (as shown in figure 11 cross-section D-D). The FEA results for section stress along the length of locking pin is obtained from a path. Maximum stress can be observed at a length of 22 mm and 38 mm. This is because at those lengths, there is an interaction between the disc and the locking pin. The locking pin of configuration 2 is less prone to structural weakness as there is addition of stiffness to

the locking pin with increase in cross sectional area. The same analogy applies for the second locking pin, where section stress along the length of locking pin 2 (as shown in figure 11 cross-section C-C) is visualized. The results are explained in figure 17 for the locking pin 2 in both configurations.

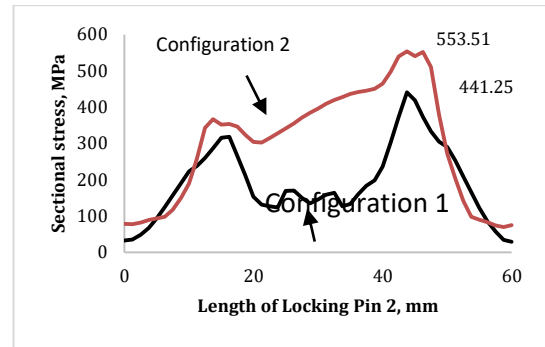


Figure 17: Section stress along the length of locking pin 2

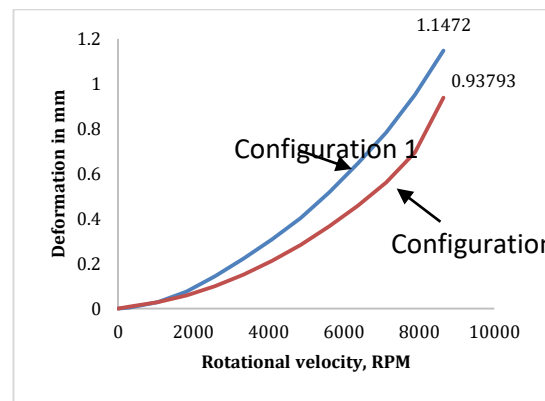


Figure 18: Radial Deformation of Closing blade

The Graphical representation of radial deformation of closing blade is as shown in figure 18. Maximum Deformation of closing blade in configuration 1 and configuration 2 is seen to be 1.14 mm and 0.93 mm respectively. The radial growth of closing blade is maximum in case of configuration 1 i.e., centers of both locking pin 1 and locking pin 2 lie on the same reference curve.

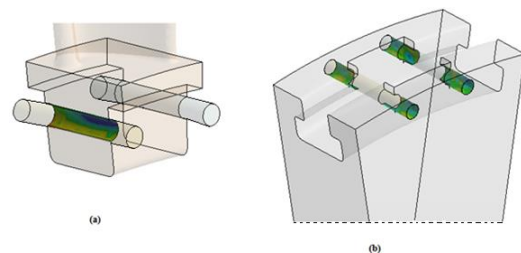


Figure 19: Bearing area (a) between pin and blade (b) between pin and disk

For configuration 1, the gross yielding stress is 101.91 MPa whereas for configuration 2, the gross yielding

stress is 37.64 MPa as shown in figure 19 a. Similarly, gross yielding stress between disc and locking pin is 135.34 MPa and 81.429 MPa as shown in figure 19 b. From both cases, it is evident that there is no localized yielding in the blade neck area and failures due to material yielding are not apparent.

Gross Yielding Stress across Critical Locations of Airfoil in the Closing Blade

The parameters affecting the stresses in airfoil of the closing blade will be considered throughout the paper since it is an industry best practice to ensure modifications in the blade do not act as stress raisers in airfoil of the blade. This is because the center of gravity is bound to change along the twist of the airfoil as position of locking pins is varied (stacking of center of gravity across multiple sections of airfoil are offset). This investigation is also carried out to check the stress distribution across the airfoil due to decrease in stiffness of closing blade. Hence it is crucial to investigate section stresses acting on various planes as shown in figure 20. Section stresses are taken for the above said conditions for a full operating speed of 8650 RPM (Rao, Peraiah *et al*, 2009). The gross yielding stress reduction at bottom span, middle span and top span is seen to be 2.7%, 0.9% and 2.4% respectively in configuration 2 compared to configuration 1. The Factor of safety of 1.34 is maintained at the bottom span, hence structural integrity of airfoil achieved.

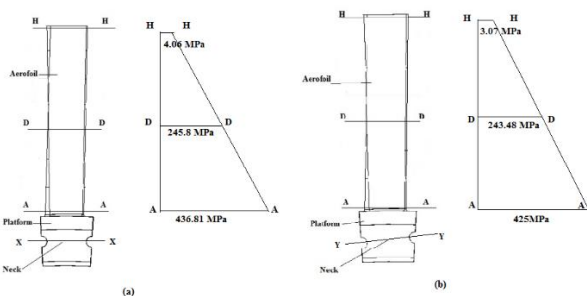


Figure 20: Section stress obtained from airfoil of closing blade (a) configuration 1 (b) configuration 2

From the figure 20 it is evident that section stresses around the bottom span of the airfoil are lowest when configuration 2 is considered. The airfoil at the bottom span is showing maximum section stress for the configuration 1.

Shear Stress Investigation

From shear perspective, the pins are subjected to shear at the disc groove region at 2 locations in each pin. The shear stress distribution in the pins is as shown in the figure 21 and 22. The force distribution that is, the double shear across the pin is shown in figure 10. The distribution of stress intensity across the pin is very clearly indicated as expected from the fundamental principles of shear.

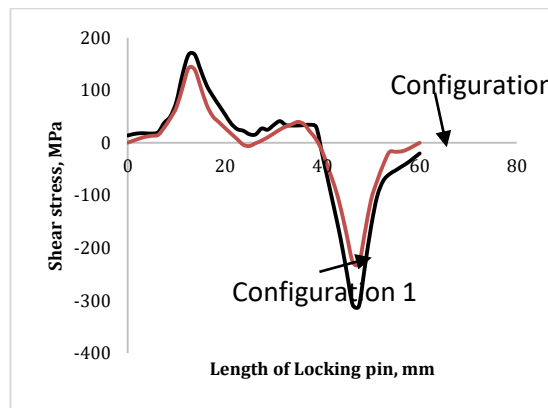


Figure 21: Shear stress along the length of locking pin 1

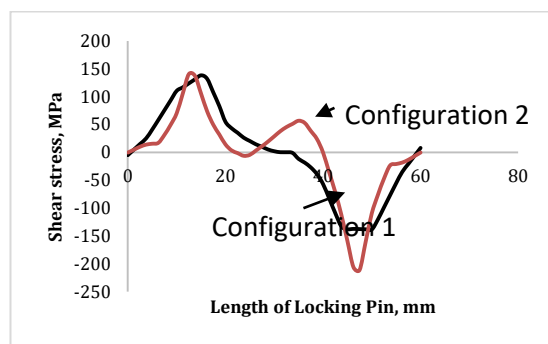


Figure 22: Shear stress along the length of locking pin 2

Conclusion

The sensitivity analysis is conducted for closing blade assembly for different loading conditions blending the classical approach. The Finite element simulation is conducted and best solution is obtained by replicating physical solutions. However, classical approach will not include geometrical nonlinearities, contact elements, manufacturing uncertainties, material nonlinearity and off design conditions. Hence, mathematical model using FEA is conducted and robust design is achieved considering all uncertainties during in-service conditions.

The theoretical classical calculations might yield a greater margin of safety because classical equations do not consider nonlinearity of material and geometry. However, FOS of FE simulation is less than expected outcome because of uncertainties present in material, manufacturing, assembly, on-site operating conditions and Non-linear kinematic analysis.

The study completely reveals the preliminary design considerations to achieve mechanical integrity in circumferential entry blades which can be considered for blade locking mechanisms. The work throws light on achieving an end to end solution for circumferential entry blades considering both bending and shear.

The local stresses of the pin which is important to maintain average section stress to prevent blade off situation from gross yielding.

The location of the pins plays a very vital role in achieving bearing stress at the blade butting area in case of T-root blades to retain bearing stress in adjacent blades apart from the closing blades.

References

- Banaszkiewicz, M. (2014). Steam turbines start-ups. Transactions of the Institute of Fluid-Flow Machinery.
- Jafarali, P., D. Krikunov, A. Mujezinović and N. A. Tisenchek (2012). Probabilistic Analysis of Turbine Blade Tolerancing and Tip Shroud Gap. ASME Turbo Expo 2012: Turbine Technical Conference and Exposition, American Society of Mechanical Engineers.
- Jaffee, R. I. (1990). Titanium steam turbine blading. Titanium Steam Turbine Blading, Elsevier: 1-25.
- Poursaeidi, E. and M. Mohammadi (2008). Failure analysis of lock-pin in a gas turbine engine. Engineering Failure Analysis 15(7): 847-855.
- Rao, J., K. C. Peraiah and U. K. Singh (2009). Estimation of dynamic stresses in last stage steam turbine blades under reverse flow conditions. Advances in Vibration Engineering, Journal of Vibration Institute of India 8(1): 71.
- Sharma, M. and R. Joshi (2001). Improvement of fretting fatigue performance of large steam turbine blade material using ball peening. Proceedings of the second International Conference on Shot Peening and Blast Cleaning (Ed. Sharma, MC), Bhopal, India.
- Tulsidas, D., M. Shantharaja and K. Kumar (2012). Design modification for fillet stresses in steam turbine blade. Int J Adv Eng Technol 3: 343-346.